Available online at www.sciencedirect.com
ScienceDirect
PLACENTA
Placenta 28 (2007) 833–840

3D Visualisation and Quantification by Microcomputed Tomography of Late Gestational Changes in the Arterial and Venous Feto-Placental Vasculature of the Mouse

M.Y. Rennie [a], K.J. Whiteley [b], S. Kulandavelu [b,c], S.L. Adamson [b,c], J.G. Sled [a,*]

[a] *Department of Medical Biophysics, University of Toronto and the Mouse Imaging Centre, Hospital for Sick Children, 555 University Avenue, Toronto, ON M5G 1X8, Canada*
[b] *Samuel Lunenfeld Research Institute at Mount Sinai Hospital, Toronto, ON M5G 1X5, Canada*
[c] *Departments of Obstetrics and Gynecology and Physiology, University of Toronto, Toronto, ON, Canada*

Accepted 18 December 2006

Abstract

This study evaluates microcomputed tomography (micro-CT) as a method to obtain quantitative three-dimensional (3D) information on the arterial and venous vasculature of the mouse placenta. Surface renderings at embryonic days (E) 13.5, 15.5, and 18.5 (full term) revealed that the arterial and venous vasculature branched within the chorionic plate whereas only the arterial vasculature deeply penetrated the placenta. Umbilical vessel diameters measured by micro-CT did not significantly differ from those measured non-invasively in vivo by ultrasound biomicroscopy. Variability in umbilical diameters, and surface area and volume measurements of arterial and venous vascular trees due to experimental error was low relative to biological variability, and significant inter-litter differences within gestational ages were detected. Furthermore, umbilical vessel diameter increased significantly and incrementally to an arterial diameter of 0.631 ± 0.009 mm and a venous diameter of 0.690 ± 0.018 mm at E18.5. Umbilical vein diameter was 3–9% greater than the artery, and both were significantly correlated with embryonic body weight ($R \geq 0.96$). Surface area and volume were determined for vessels greater than the minimum resolvable diameter of 0.03 mm which therefore excluded capillaries. Arterial surface area and volume were unchanged from E13.5–15.5 but then more than doubled at E18.5 (to 170 ± 13 mm^2 and 7.2 ± 0.8 mm^3, respectively). Venous surface areas and volumes changed similarly with development although surface areas were lower than their arterial counterparts. We conclude that micro-CT has sufficient accuracy and precision to quantify late gestational changes in the 3D structure of the arterial and venous vasculature of the mouse placenta.

Keywords: Feto-placental vasculature; Mouse; Microcomputed tomography; Imaging; Perfusion

1. Introduction

Genetically altered mice are proving valuable models for advancing our understanding of placental development. Indeed, our understanding of the genetic regulation of branching morphogenesis and vascularisation of the placenta [1,2] has been rapidly advanced by the use of mice with targeted mutations. More than 60 genes have been shown to play a role in these processes [2]. Importantly, many genes expressed during placental development in mice often have homologues that are similarly expressed in the human placenta [1–3]. Furthermore, the value of the mouse as a model for placental research is enhanced by the strong structural and cellular similarities between the placentas of the two species [3–5].

Vascular corrosion casts of the feto-placental circulation have shown remarkable similarity between the feto-placental circulation in the mouse placenta [5] and in a single lobule of

* Corresponding author. Tel.: +1 416 813 7654x1438; fax: +1 416 813 2208.
E-mail address: jgsled@sickkids.ca (J.G. Sled).

0143-4004/$ - see front matter © 2007 Elsevier Ltd. All rights reserved.
doi:10.1016/j.placenta.2006.12.005

the human placenta [6]. In both species, the umbilical cord vessels enter the discoid-shaped placenta near the centre and branch extensively over the chorionic surface sending smaller diameter vessels deep into the placenta to supply the richly capillarised terminal vascular bed where exchange with maternal blood occurs. Although similar in structure and function, this exchange region is referred to as the placental villous tree in humans and the placental labyrinth in mice. Given the strong similarities in the feto-placental vasculatures, mutant mouse models could provide insight into the mechanisms that underlie feto-placental hypovascularisation in fetal intrauterine growth restriction in human pregnancy [7–9].

However, progress in understanding the genetic regulation of feto-placental vascular development has been hampered by inadequate methods for identifying and quantifying the specific nature of the feto-placental vascular defect. Vascular corrosion casts provide immediate 3D visualisation of this vasculature [5] but obtaining quantitative data from casts is cumbersome and superficial vasculature obscures deeper structures. Stereology of histological sections has been used to obtain quantitative 3D measures of placental vascularity [10,11] but sectioning permanently destroys the connectivity between vessels and hence the overall topology. Thus, stereology is not well suited to providing information on vascular branching patterns or on the serial versus parallel arrangement of vessels.

Microcomputed tomography (micro-CT), an X-ray imaging modality, provides the means for obtaining this information through 3D quantification of vascular beds. Micro-CT has been established as a leading method in small animal imaging of vascular beds [12,13], where its high resolution and large specimen coverage provide a detailed view of the microcirculation suitable for structural analysis and blood flow modelling [14]. Despite these advantages, this technique has not been utilised in the study of the murine placenta.

Thus, in the current study we evaluated micro-CT as a method for 3D visualisation and quantification of the feto-placental circulation of the mouse. Currently, capillaries $<20\,\mu m$ in diameter cannot be visualised with tabletop micro-CT systems [12,13]; however, we expected that most vessels at the critical arteriolar level of the circulation where vascular resistance and flow regulation reside [15] would be detected. Preliminary studies showed that the arterial and venous vessels within the chorionic plate were often in such close proximity that the space between them could not be resolved and this impeded quantitative analysis. Thus, our first objective was to evaluate the technical success rate for independent visualisations of the arterial or venous feto-placental vasculatures. We then evaluated the accuracy and reproducibility of 3D quantification of umbilical vessel diameters, and the surface area and volume of the vasculature. Finally, we determined whether the method could detect and quantify the elaboration of the feto-placental vasculature that was anticipated to occur during late-gestational development.

2. Materials and methods

2.1. Mice

Experimental procedures were approved by the Animal Care Committee of Mount Sinai Hospital and conducted in accordance with guidelines established by the Canadian Council on Animal Care. CD-1 mice, a common outbred laboratory strain, were purchased from Charles River Laboratories (Montreal, QC) and housed under specific-pathogen free conditions. Males were mated in-house with virgin females aged 10–12 weeks. The morning that a vaginal copulation plug was detected was designated embryonic day (E) 0.5. Pregnant mice were killed by cervical dislocation at E13.5, E15.5, or E18.5 (full term in this strain) and their uteri quickly removed and immersed in ice-cold phosphate buffered saline (PBS).

2.2. Injection of contrast agent

The feto-placental vasculature was perfused with an X-ray contrast agent using a method previously developed to perfuse placentas for vascular corrosion casting [5,16]. Briefly, the uterus was cut between individual implantation sites and the segment was weighed. The embryo and placenta were surgically exposed and bathed in warm PBS to resume cardiac function and placental blood flow. A double-lumen tapered glass cannula [16] was advanced into either the umbilical artery or vein with the alternate vessel nicked to serve as a vent. All cord insertions were centrally located in the placenta of all implantation sites dissected in this study. Warm 2% xylocaine in 0.9% NaCl and 100 IU heparin/ml was perfused through the cannula to clear blood from the vasculature. The radio-opaque silicone rubber contrast agent (Microfil, Flow Tech Inc., Carver, MA) was then infused into either the arterial vasculature via the umbilical artery, or the venous vasculature via the umbilical vein until its bright yellow colour could be clearly seen in the capillary bed, at which point the umbilical cord was tied off and the cannula removed. In this manner, separate arterial or venous specimens were obtained. After infusion, the silicone rubber was allowed to polymerise before the umbilical cord was severed, placental and embryonic weights were recorded, and the placenta was immersed in fixative (10% buffered formalin phosphate) for 24–48 h at 4 °C. Specimens were mounted in 1% agar made with 10% formalin in preparation for scanning.

We initially acquired and analysed eight arterial specimens from each of two litters at E15.5 and found significant inter-litter variation (analysis not shown). Therefore to assess placental vascular growth in late gestation, two arterial and two venous specimens per litter were obtained from four litters at each of three time points (E13.5, E15.5, E18.5). This allowed inter- and intra-litter variation to be quantified. The two initial litters of eight arterial specimens were included in the results augmenting our arterial sample size at E15.5. Sixty-four specimens in all were analysed.

2.3. Image acquisition and processing

3D datasets were acquired for each specimen using an MS-9 micro-CT scanner (GE Medical Systems, London, ON). The performance of this specimen scanning system has previously been evaluated and described by Marxen et al. [13], who found a maximum resolution of 38 line pairs/mm at 10% contrast based on the modulation transfer function. In practice, this allows for visualisation and measurement of vessels greater than 30 μm. With the X-ray source at 80 kVp and 80 μA, and the specimen positioned for a magnification of 3.47×, each specimen was rotated 360° around the vertical axis, generating 720 views in 2 h. These views were reconstructed using the Feldkamp algorithm [17] for cone beam CT. The resulting 3D data block contained $500 \times 500 \times 500$ 13 μm voxel elements.

A surface corresponding to the intensity contours at a threshold (1500–2500 HU) halfway between the intensity of tissue and that of the injected contrast agent was constructed for each dataset. Represented internally as a mesh of more than a million adjacent polygons with edge lengths on the order of a voxel (13 μm), this surface allowed 3D visualisation of the placental vasculature as well as calculation of vessel diameters, surface area, and overall lumen volume. The iso-intensity surface constructions and geometric

measurements were made using the Amira software package (TGS Inc, Berlin, Germany).

2.4. Evaluation of method

Segments of polyethylene tubing (Intramedic, Becton Dickinson, Sparks, MD) with manufacturer specified internal diameters of 0.279, 0.381, 0.584, and 0.760 mm were imaged with and without Microfil in the lumen. Filled and unfilled diameters were compared to assess dimensional stability (i.e. shrinkage), and unfilled diameters were compared with the manufacturer's specifications to assess accuracy. Accuracy was further assessed by comparing umbilical arterial and venous diameter measurements obtained non-invasively in vivo using ultrasound biomicroscopy (Vevo 770, Visualsonics Inc., Toronto, ON) with those obtained by micro-CT. 30 MHz ultrasound was used to image the umbilical vasculature of 11 embryos at E13.5 and 13 embryos at E15.5 from three isoflurane-anaesthetised pregnant mice at each age. Umbilical vessel diameters were measured from power Doppler images using digital callipers and results at each age were averaged.

The reproducibility of the micro-CT technique itself was assessed by determining the coefficient of variability of four scan/analysis repetitions for one E18.5 arterial and one E18.5 venous specimen. Sensitivity was evaluated by determining the smallest vessel observed in a given scan.

2.5. Statistical testing

We estimated a mixed effect linear model using the LME package from the R statistical software (www.r-project.org) [18]. This package provides analysis of variance for random and fixed effects and *t*-tests for the marginal distributions corresponding to the columns of the linear model. A fixed effect model was used to determine if interactions between vessel type (artery or vein) and gestational age were significant. We moved to a mixed effect model to evaluate the addition of inter-litter variation as a random factor and used likelihood ratios to test whether inter-litter variation needed to be independently modelled for arteries and veins. ANOVA was used to assess whether there was a significant effect of our fixed factors, vessel type and gestational age. *t*-tests were used to assess differences between ages based on the mixed effects model. Results are presented as the mean ± SE where n is the number of perfused specimens examined by micro-CT. $P < 0.05$ was considered significant.

3. Results

Successful vascular surface renderings were obtained from 47% (83 of 176) of placentas in which perfusion with contrast agent was attempted. The vast majority of failures were due to problems identified during the perfusion procedure so that 87 of 176 placentas were rejected prior to imaging due to inadequate or inappropriate filling (e.g. segments of the placenta remained unperfused, vessel ruptures caused leakage, or contrast agent passed through the capillaries and entered the unintended vasculature). Only 6 of 176 (3%) were rejected following vascular reconstruction and surface rendering. These were rejected when there were small gaps in otherwise filled vessels, or the contrast agent had leaked, or there were unfilled portions of the vasculature (Fig. 1). Perfusion failures tended to occur more frequently at E13.5 at which age the umbilical vessels were smallest and most fragile, and at E18.5 because the feto-placental vasculature sometimes failed to fully vasodilate with warming and the resumption of placental blood flow. Interestingly, vasospasm was only observed in some pregnant mice at E18.5 and, when observed, it affected

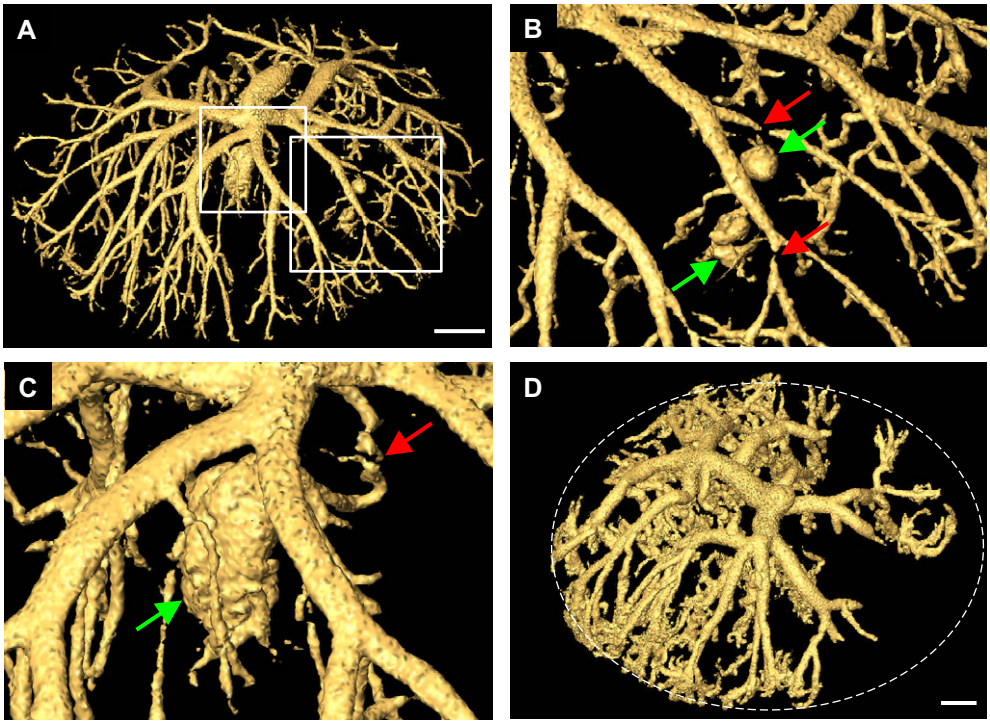

Fig. 1. Examples of iso-intensity surface renderings excluded from analysis. (A) Arterial surface rendering at 13.5 days gestation. Boxed regions are enlarged in (B) and (C). This surface rendering shows small gaps in otherwise filled vessels (e.g. red arrows in B,C) and apparent leaks from ruptured vasculature (e.g. green arrows in B,C) to illustrate artifacts that resulted in rejection of perfused specimens at the imaging stage. (D) Renderings in which vasospasm prevented portions of the vasculature from filling with contrast agent, as in this E18.5 example, were also excluded. Note sparseness of vasculature and blunt ends of large vessels towards the right in the area demarked by the dashed line. Scale bars, 0.5 mm.

the entire litter. The study protocol required two arterial and two venous specimens per litter. Litters with too few acceptable specimens were excluded, as were placentas collected in addition to the two arterial and venous specimens required. This resulted in 64 of 83 acceptable specimens being included in the final analysis.

Visualisation of the 3D vascular iso-intensity surfaces of the arterial and venous placental specimens suggested that both aspects of the circulation became larger and more highly branched as gestation advanced (Fig. 2). During the placental perfusion procedure, we observed that the single umbilical artery and single umbilical vein branched extensively at the chorionic surface with the arterial branches located beneath those of the more superficial venous vasculature. The site of penetration of the umbilical artery divided the large veins into two trees which, from surface renderings, were observed to exhibit a magistral/mixed branching pattern (Fig. 2). Examination of surface renderings also showed that the branching pattern of the arterial tree was largely dichotomous (Fig. 2), and that the relatively evenly distributed smaller arteries and arterioles in the placenta exhibited a concave curvature to the distal surface that was more prominent later in gestation (Fig. 3). This can be better appreciated in the online supplemental movie where the surface rendering shown in Fig. 2C is rotated through 360°. The smallest branches resolvable were approximately 0.03 mm in diameter. Capillaries appeared as an indistinct mass with an intensity much below the threshold used to construct the iso-intensity surfaces and thus were not visualised.

Quantitative information on umbilical vessel diameters was obtained by manually measuring the iso-intensity surface of imaged placental specimens using a digital calliper. To evaluate measurement accuracy, tubing of known calibre was filled with contrast agent and then imaged. For tubing with manufacturer specified internal diameters of 0.279 to 0.760 mm, diameters obtained by micro-CT were within 0.010 mm and thus less than the width of one image voxel (0.013 mm). In addition, diameter measurements of the contrast agent within filled tubing were within 0.020 mm of the unfilled diameter suggesting that no appreciable contrast agent shrinkage had occurred. Umbilical vessel diameters measured using ultrasound biomicroscopy non-invasively in vivo in a separate series of pregnant mice of the same strain revealed diameters which did not significantly differ from those measured by micro-CT (Table 1). These results suggest that quantitative diameter information obtained by micro-CT is accurate and is similar to the in vivo state.

Variability introduced by the micro-CT method was assessed by performing repeated scans, reconstructions, and quantitative analysis of iso-intensity surfaces of the same arterial and venous specimen. The coefficient of variation for umbilical diameters was $<1\%$, for surface area was $\leq 2\%$, and for volume was $<6\%$. Analysis by ANOVA showed that the method was also sufficiently reproducible to detect statistically significant differences in umbilical vessel diameters, and vascular surface areas and volumes between litters at the same gestational age. Intra-litter standard deviation, which incorporates true intra-litter variation and experimental error, was similar to the standard deviation of within litter means (i.e. the inter-litter standard deviation in Table 2). Hence specimens selected from different litters have approximately double the variation of those selected from a single litter. Overall, variability caused by experimental error was small relative to biologic variability. Thus, the method was considered adequate for quantification of the arterial and venous placental vasculatures.

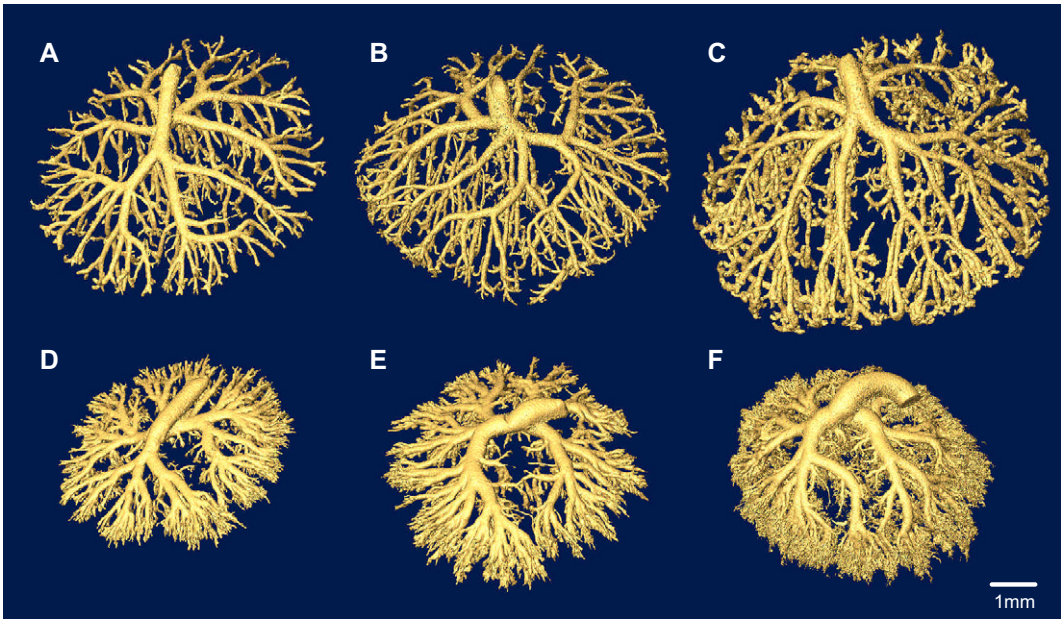

Fig. 2. Iso-intensity surface renderings of arterial (A–C) and venous (D–F) fetoplacental vascular trees from E13.5 (A,D), E15.5 (B,E) and E18.5 (C,F). The supplemental movie http://www.mouseimaging.ca/papers/rennie2006/placenta.mov shows the surface rendering in panel C rotating through 360° as an example of 3D visualisation. Scale, 1 mm.

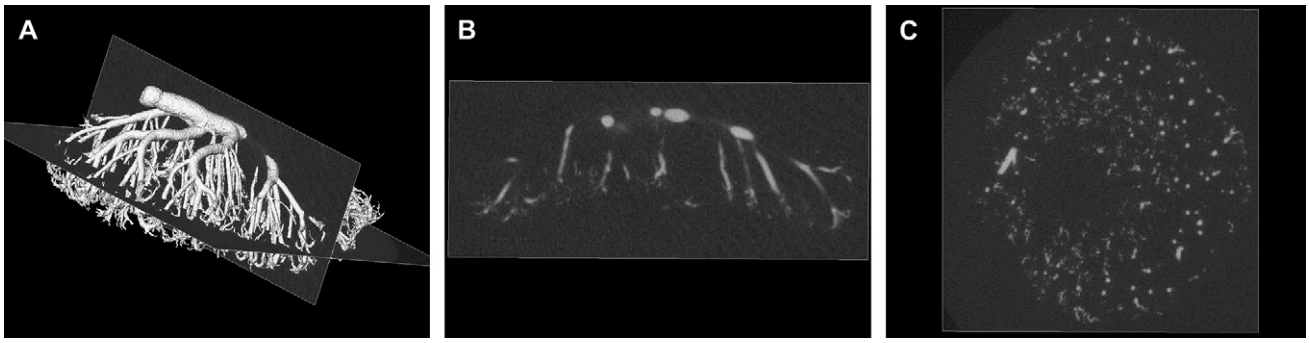

Fig. 3. (A) Iso-intensity surface rendering of an E15.5 arterial vascular tree with two orthogonal planes illustrating sample cuts through the data set. (B) Plane perpendicular to the chorionic plate showing larger arteries on the chorionic surface and smaller arteries and arterioles penetrating deeply into the placenta. (C) Plane parallel to the chorionic plate showing the relatively even distribution of arteries and arterioles across the placenta. The gap in the vasculature near the middle of the image is caused by the concave curvature of the distal surface of the placenta which is visible in (B).

Quantitative analysis of iso-intensity surfaces revealed significant increases in umbilical artery and vein diameters with increasing gestational age, and that umbilical vein diameter was slightly but significantly greater than umbilical artery diameter by 3–9% at each age (Fig. 4). Umbilical vessel diameter was significantly correlated with embryo weight over the age range studied (Pearson's correlation coefficients were 0.96 for arterial diameter, and 0.97 for the vein) (Fig. 5). Interestingly, despite the incremental increases in umbilical vessel diameter with age, vascular surface area and volume showed no significant change between E13.5 and E15.5 and then more than doubled at E18.5 (Fig. 4). At all ages, the vascular surface area of the arterial vascular tree was significantly greater than that of the venous tree (by 22–40%). In contrast, arterial and venous vascular volumes were not significantly different (Fig. 4).

4. Discussion

The results of this study show that micro-CT imaging and analysis of the feto-placental vasculature provide intuitive 3D visualisations of the vascular bed as well as quantitative data that are precise relative to normal biological variation and, based on umbilical vessel diameters, close to in vivo measurements. Furthermore, quantification of the iso-intensity surfaces yielded novel findings. We found that the diameters of the umbilical artery and vein were similar. Both increased incrementally from E13.5 to term in accord with the increase in embryonic body weight, but total vascular surface area and volume increased more rapidly in the final days of gestation. These results show the utility of micro-CT for understanding and quantifying the feto-placental circulation of the mouse during normal development and also suggest its use for quantitative evaluation of feto-placental defects in genetically-altered mice.

The umbilical artery and vein form between E8.5 and E9.5 of gestation in the mouse by vasculogenesis within the allantois when it transforms into the umbilical cord [19,20]. As gestation advances, peak systolic blood flow velocity first detected at E9.5 progressively increases in the umbilical artery and vein [21–23]. The diameters of both vessels also progressively increase [23] such that calculated umbilical blood flow increases in proportion to embryonic weight [23]. Our results further show that the diameters of the umbilical vessels continue to increase to term, and that vessel calibre is highly correlated with, although not proportional to, embryonic weight. We also found that umbilical artery and vein diameters are remarkably similar; veins/venules are generally larger than the corresponding arteries/arterioles in the postnatal vasculature (e.g. [15,24,25]) and this difference in calibre is thought to be mediated by pressure sensitivity of the shear stress–vessel diameter relationship [15]. Despite this unusual similarity in calibre, the arterial and venous vasculatures exhibited profoundly different branching patterns, with the venous vasculature confined to the proximal chorionic surface and the arteries branching deeply into the placenta below. Also, veins exhibited a much more abrupt transition from large branch vessels to small terminal vessels which may account for their lower surface area yet similar volume.

Whereas there were incremental increases in umbilical vessel diameter, vascular surface area and volume of the feto-placental arterial and venous vascular trees increased rapidly

Table 1
Umbilical diameters measured using micro-CT or ultrasound

	Umbilical artery diameter (mm)		Umbilical vein diameter (mm)	
	E13.5	E15.5	E13.5	E15.5
Micro-CT	0.377 ± 0.008 ($n = 8$)	0.483 ± 0.004 ($n = 8$)	0.400 ± 0.014 ($n = 7$)	0.498 ± 0.009 ($n = 6$)
Ultrasound	0.396 ± 0.005 ($n = 11$)	0.479 ± 0.004 ($n = 13$)	0.410 ± 0.004 ($n = 11$)	0.510 ± 0.010 ($n = 13$)
ANOVA P	0.054	0.504	0.355	0.611

Results shown as mean ± SE where n = number of specimens for micro-CT and number of embryos for ultrasound.

Table 2
ANOVA inter- and intra-litter standard deviation (SD) shown as "SD (95% confidence interval)"

	Umbilical diameter SD (mm)	Surface area SD (mm^2)	Volume SD (mm^3)
Arterial inter-litter variation	0.017 (0.009–0.032)	20 (11–36)	0.5 (0.1–2.7)
Venous inter-litter variation	0.030 (0.017–0.054)	15 (7–33)	0.6 (0.1–2.7)
Residual variation (Intra-litter variation + experimental error)	0.021 (0.016–0.053)	17 (13–21)	1.5 (1.2–1.8)

Inter- and intra-litter standard deviations were not significantly different.

in the final days of gestation. This novel finding may be explained by changes in the feto-placental capillaries that they supply. Using stereology, Coan and colleagues [10] found that total capillary length did not significantly change between E12.5 and E14.5 but then increased progressively to term, whereas total surface area increased rapidly between E12.5 and E16.5 at the same time as mean capillary diameter decreased (from ~0.014 to ~0.011 mm). The latter change in capillary structure therefore appears to coincide with the rapid increase in surface areas and volumes of the larger vessels of the placenta observed in the current study. Interestingly, this late gestational remodelling of the feto-placental circulation also coincides with a marked change in feto-placental hemodynamics. On or after E15.5, a non-zero Doppler diastolic blood velocity first appears then diastolic velocity progressively increases to term in the umbilical artery of the mouse embryo [22]. It is tempting to speculate that the hemodynamic change may be caused by the coincident structural changes in the feto-placental vasculature.

There are limited data in the literature with which to compare our quantitative results. Micro-CT imaging and quantification of the term human placental vasculature has been performed [26] but, unlike the current study, a sample of the whole organ was analysed so surface areas and volumes are expressed per unit volume of the sample, and surface areas and volumes included the complete vasculature (arteries, veins, and capillaries) so results are difficult to compare with those of the current study. Similarly, umbilical vascular diameters have been assessed in human pregnancy [27] but the human has two arteries and one vein in the cord (in contrast to the single artery and vein in the mouse) which may account for the dissimilar umbilical vessel calibres in humans. In C57Bl6 mouse embryos, quantitative information on total volumes and surface areas of feto-placental capillaries by stereology is available and comparison with our results reveals that the total volume of the capillaries (~2 to 14 mm^3 from E12.5 to E18.5 [10]) is similar in magnitude to that of the arterial or venous vasculatures of CD-1 embryos (~2 to 7 mm^3 from E13.5 to E18.5) whereas, consistent with the exchange function of the capillaries, the total capillary surface area (~2000 to 27,000 mm^2 from E12.5 to E18.5) is much greater than that of the arterial or venous vasculatures (~70 to 160 mm^2 from E13.5 to E18.5) of the current study. Capillary volumes and surface areas in C57Bl6 mice likely underestimate those of CD-1 mice due to their smaller placental size (placental weight ~33% less than CD-1).

Our evaluation revealed significant strengths of the micro-CT technique for examining the feto-placental circulation of the mouse. Strengths of the method include (1) the ability to include the entire placenta in a single dataset thereby avoiding sampling errors and the necessity of extrapolating to obtain results for the entire organ, (2) the vasculature is protected from damage and supported in its in situ configuration, (3) the tissue remains intact for later histological analysis, (4) contrast agent shrinkage is minimal facilitating comparison with in vivo data, and (5) vessels as small as small arterioles (down to 0.030 mm), representing most resistance arterioles [15], are detected. Other strengths include that quantification of umbilical diameter, and surface area and volume of the feto-placental vasculature was highly reproducible, and that it was feasible to obtain specimens with selective filling of either the arterial or the venous circulations. The latter greatly

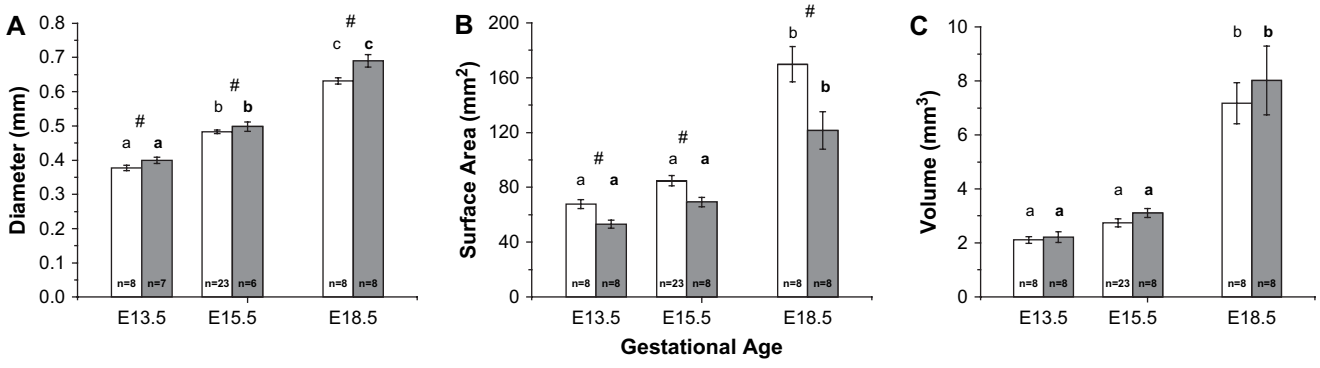

Fig. 4. Developmental changes in the arterial (open bars) and venous (shaded bars) vasculatures of the fetoplacental circulation. (A) Arterial and venous umbilical diameter, (B) surface area, and (C) volume of the arterial and venous vasculatures are shown as mean ± SE. Sample size (*n*) is less than 8 in cases where the umbilical cord was tied off too close to the chorionic plate to allow vessel diameter measurements. Different letters indicate significant differences within vessel type with age, # indicates significant differences between vessel types at the same age.

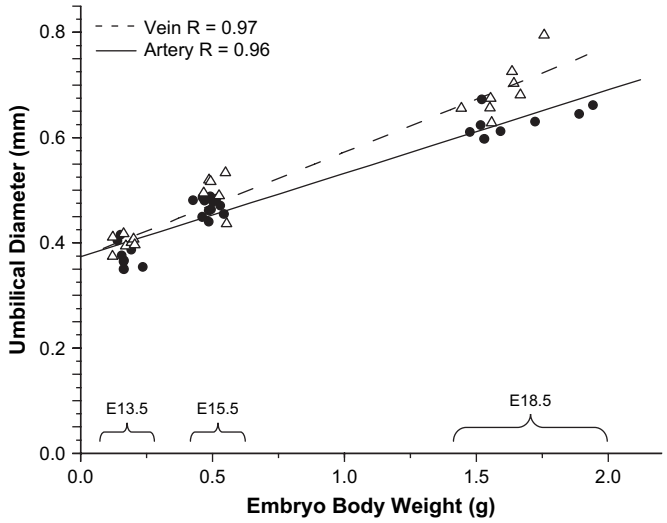

Fig. 5. Linear relationship between umbilical artery diameter (solid circles) or umbilical vein diameter (open triangles) and embryonic body weight. Embryo was isolated and the wet weight obtained after contrast agent infusion into the placental circulation. Each point corresponds to a specimen from Fig. 4. R = Pearson's correlation coefficient.

simplifies analysis as compared to image processing techniques for retrospectively segmenting arteries from veins [14].

The micro-CT technique also had limitations for studies of the mouse placenta. The technique was most feasible late in gestation due to the relative difficulty of performing feto-placental perfusion at earlier gestational ages. In our study, we were not able to resolve the smallest arterioles and venules, and capillaries. Although these vessels can be resolved with higher resolution instruments, such instruments typically have specimen size constraints that may preclude analysis of the entire placenta. A recent report images the entire mouse brain with arteriole scale resolution and a portion with capillary resolution then merges the datasets at the analysis stage [28]. A similar approach applied to the feto-placental vasculature could be used to extend analysis to include all vessels. The necessity of perfusing vessels with a contrast agent for visualisation means that complete homogeneous filling of every vessel cannot be guaranteed, a limitation shared by many other methods. However, almost all problems of this nature were apparent at the perfusion stage because the bright yellow contrast agent was highly visible within the feto-placental vasculature. Only a few specimens were rejected after imaging when abruptly ending large vessels and gaps in the otherwise even and symmetrical placental vasculature were observed. Whether more subtle filling artifacts may be revealed by more detailed image analysis is not currently known. Our contrast agent is not compatible with the tissue maceration required for a direct comparison between micro-CT scanned and corrosion casted specimens; however, a recent paper compares optical and micro-CT images of a macerated specimen side-by-side [29]. With the method described here, intravascular pressure was unknown and pressure could influence vessel calibre. However, our experience suggests that once the vessels are inflated (i.e. vessels appear round rather than flattened) there is no visible distension of superficial vessels as pressure is slowly increased. Before vascular distension was discernable, a vascular rupture and leak would eliminate the specimen from the study. Thus, there appeared to be little elasticity at this early stage of development, at least in the visible superficial vasculature. We used the combination of heat, xylocaine in the perfusate, and the embryonic blood circulating through the feto-placental vasculature to re-dilate the feto-placental circulation in an attempt to reproduce the nearly maximally-dilated in vivo state that characterises this bed [30,31]. Vasospasm at term could not be eliminated by this method therefore resulting in the rejection of some specimens. However, the high level of agreement between in vivo umbilical arterial and venous diameters, and the low intra-litter variability of acceptable specimens supports the validity of this approach.

The use of micro-CT is not limited to the placental circulation; recent studies have used it to examine the lung [32], liver [32], kidney [33], brain [34], and heart [35]. This flexibility allows for comparative studies between vascular beds as well as comparisons with mutated lines, the latter in some cases showing radical differences [36]. When used in combination with software for automatic detection and measurement of vessels [37], the overall pattern of a vascular bed can be characterised in a statistical manner [14], and this information can be used to determine vascular flows, resistances, and pressure gradients throughout the bed. Indeed a recent paper demonstrated excellent agreement between calculated flows and micro-sphere based flow measurements in the rat kidney [29]. Together these technical developments suggest that physiologically important data can be extracted from micro-CT datasets. This method will therefore provide a powerful tool for detailed study of changes in the structure and hemodynamics of the mouse placenta during normal development and in response to genetic perturbations.

In conclusion, the application of micro-CT imaging and analysis to the feto-placental circulation of the mouse has been rigorously evaluated. The method was found to generate data with sufficient accuracy and reproducibility to reveal novel quantitative information on the late gestational development of the arterial and venous feto-placental vasculatures. We suggest this method will prove useful in future studies on genetically altered mouse models for qualitative and quantitative evaluation of abnormalities in the feto-placental vasculature.

Acknowledgement

This research was supported by the Heart and Stroke Foundation of Ontario, Grant No. NA5804.

References

[1] Sapin V, Blanchon L, Serre AF, Lemery D, Dastugue B, Ward SJ. Use of transgenic mice model for understanding the placentation: towards clinical applications in human obstetrical pathologies? Transgenic Res 2001;10:377–98.

[2] Watson ED, Cross JC. Development of structures and transport functions in the mouse placenta. Physiology (Bethesda) 2005;20:180–93.

[3] Cross JC, Baczyk D, Dobric N, Hemberger M, Hughes M, Simmons DG, et al. Genes, development and evolution of the placenta. Placenta 2003;24:123–30.
[4] Georgiades P, Ferguson-Smith AC, Burton GJ. Comparative developmental anatomy of the murine and human definitive placentae. Placenta 2002;23:3–19.
[5] Adamson SL, Lu Y, Whiteley KJ, Holmyard D, Hemberger M, Pfarrer C, et al. Interactions between trophoblast cells and the maternal and fetal circulation in the mouse placenta. Dev Biol 2002;250:358–73.
[6] Benirschke K, Kaufmann P, Baergen RN. Pathology of the human placenta. 5th ed. Berlin: Springer; 2006.
[7] Krebs C, Macara LM, Leiser R, Bowman AW, Greer IA, Kingdom JC. Intrauterine growth restriction with absent end-diastolic flow velocity in the umbilical artery is associated with maldevelopment of the placental terminal villous tree. Am J Obstet Gynecol 1996;175:1534–42.
[8] Macara L, Kingdom JC, Kohnen G, Bowman AW, Greer IA, Kaufmann P. Elaboration of stem villous vessels in growth restricted pregnancies with abnormal umbilical artery Doppler waveforms. Br J Obstet Gynaecol 1995;102:807–12.
[9] Jackson MR, Walsh AJ, Morrow RJ, Mullen JB, Lye SJ, Ritchie JW. Reduced placental villous tree elaboration in small-for-gestational-age pregnancies: relationship with umbilical artery Doppler waveforms. Am J Obstet Gynecol 1995;172:518–25.
[10] Coan PM, Ferguson-Smith AC, Burton GJ. Developmental dynamics of the definitive mouse placenta assessed by stereology. Biol Reprod 2004;70:1806–13.
[11] Mayhew TM. Stereology and the Placenta: Where's the point?—a review. Placenta 2006;27(Suppl):17–25.
[12] Bentley MD, Ortiz MC, Ritman EL, Romero JC. The use of microcomputed tomography to study microvasculature in small rodents. Am J Physiol Regul Integr Comp Physiol 2002;282:R1267–79.
[13] Marxen M, Thornton MM, Chiarot CB, Klement G, Koprivnikar J, Sled JG, et al. MicroCT scanner performance and considerations for vascular specimen imaging. Med Phys 2004;31:305–13.
[14] Sled JG, Marxen M, Henkelman RM. Analysis of micro-vasculature in whole kidney specimens using micro-CT. In 2004.
[15] Pries AR, Secomb TW, Gaehtgens P. Design principles of vascular beds. Circ Res 1995;77:1017–23.
[16] Whiteley KJ, Pfarrer CD, Adamson SL. Vascular corrosion casting of the uteroplacental and fetoplacental vasculature in mice. Methods Mol Med 2006;121:371–92.
[17] Feldkamp LA, Kress JW. Practical cone-beam algorithm. J Opt Soc Am 1984;1:612–9.
[18] Pinheiro JC, Bates DM. Mixed-effects models in S and S-PLUS. New York: Springer; 2000.
[19] Cross JC, Simmons DG, Watson ED. Chorioallantoic morphogenesis and formation of the placental villous tree. Ann N Y Acad Sci 2003;995:84–93.
[20] Downs KM, Gifford S, Blahnik M, Gardner RL. Vascularization in the murine allantois occurs by vasculogenesis without accompanying erythropoiesis. Development 1998;125:4507–20.
[21] Phoon CK, Aristizabal O, Turnbull DH. 40 MHz Doppler characterization of umbilical and dorsal aortic blood flow in the early mouse embryo. Ultrasound Med Biol 2000;26:1275–83.
[22] Mu J, Adamson SL. Developmental changes in hemodynamics of the uterine artery, the utero- and umbilico-placental, and vitelline circulations in the mouse throughout gestation. Am J Physiol Heart Circ Physiol 2006; 291(3):H1421–8.
[23] MacLennan MJ, Keller BB. Umbilical arterial blood flow in the mouse embryo during development and following acutely increased heart rate. Ultrasound Med Biol 1999;25:361–70.
[24] Nordsletten DA, Blackett S, Bentley MD, Ritman EL, Smith NP. Structural morphology of renal vasculature. Am J Physiol Heart Circ Physiol 2006;291:H296–309.
[25] Duvernoy HM, Delon S, Vannson JL. Cortical blood vessels of the human brain. Brain Res Bull 1981;7:519–79.
[26] Langheinrich AC, Wienhard J, Vormann S, Hau B, Bohle RM, Zygmunt M. Analysis of the fetal placental vascular tree by X-ray micro-computed tomography. Placenta 2004;25:95–100.
[27] Weissman A, Jakobi P, Bronshtein M, Goldstein I. Sonographic measurements of the umbilical cord and vessels during normal pregnancies. J Ultrasound Med 1994;13:11–4.
[28] Heinzer S, Krucker T, Stampanoni M, Abela R, Meyer EP, Schuler A, et al. Hierarchical microimaging for multiscale analysis of large vascular networks. Neuroimage 2006;32:626–36.
[29] Marxen M, Sled JG, Yu LX, Paget C, Henkelman RM. Comparing microsphere deposition and flow modeling in 3D vascular trees. Am J Physiol Heart Circ Physiol 2006;291:H2136–41.
[30] Dusseau JW, Hutchins PM, Malbasa DS. Stimulation of angiogenesis by adenosine on the chick chorioallantoic membrane. Circ Res 1986;59: 163–70.
[31] Paulick RP, Meyers RL, Rudolph AM. Vascular responses of umbilical-placental circulation to vasodilators in fetal lambs. Am J Physiol 1991;261:H9–14.
[32] Ritman EL. Micro-computed tomography of the lungs and pulmonary-vascular system. Proc Am Thorac Soc 2005;2:477–80. 501.
[33] Ortiz MC, Garcia-Sanz A, Bentley MD, Fortepiani LA, Garcia-Estan J, Ritman EL, et al. Microcomputed tomography of kidneys following chronic bile duct ligation. Kidney Int 2000;58:1632–40.
[34] Krucker T, Lang A, Meyer EP. New polyurethane-based material for vascular corrosion casting with improved physical and imaging characteristics. Microsc Res Tech 2006;69:138–47.
[35] Clauss SB, Walker DL, Kirby ML, Schimel D, Lo CW. Patterning of coronary arteries in wildtype and connexin43 knockout mice. Dev Dyn 2006;235:2786–94.
[36] Ward NL, Haninec AL, Van SP, Sled JG, Sturk C, Henkelman RM, et al. Angiopoietin-1 causes reversible degradation of the portal microcirculation in mice: implications for treatment of liver disease. Am J Pathol 2004;165:889–99.
[37] Fridman Y, Pizer SM, Aylward S, Bullitt E. Extracting branching tubular object geometry via cores. Med Image Anal 2004;8:169–76.